Suppression of bursting synchronization in clustered scale-free (rich-club) neuronal networks

E. L. Lameu,[1] C. A. S. Batista,[2] A. M. Batista,[3] K. Iarosz,[1] R. L. Viana,[2,a)] S. R. Lopes,[2] and J. Kurths[4]
[1]*Graduate Program in Physics, State University of Ponta Grossa, Ponta Grossa, Paraná, Brazil*
[2]*Departament of Physics, Federal University of Parana, Curitiba, Paraná, Brazil*
[3]*Departament of Mathematics and Statistics, State University of Ponta Grossa, Ponta Grossa, Paraná, Brazil*
[4]*Department of Physics, Humboldt University, Berlin, Germany; Institute for Complex Systems and Mathematical Biology, Aberdeen, Scotland; and Potsdam Institute for Climate Impact Research, Potsdam, Germany*

(Received 17 October 2012; accepted 5 December 2012; published online 28 December 2012)

Functional brain networks are composed of cortical areas that are anatomically and functionally connected. One of the cortical networks for which more information is available in the literature is the cat cerebral cortex. Statistical analyses of the latter suggest that its structure can be described as a clustered network, in which each cluster is a scale-free network possessing highly connected hubs. Those hubs are, on their hand, connected together in a strong fashion ("rich-club" network). We have built a clustered scale-free network inspired in the cat cortex structure so as to study their dynamical properties. In this article, we focus on the synchronization of bursting activity of the cortical areas and how it can be suppressed by means of neuron deactivation through suitably applied light pulses. We show that it is possible to effectively suppress bursting synchronization by acting on a single, yet suitably chosen neuron, as long as it is highly connected, thanks to the "rich-club" structure of the network. © *2012 American Institute of Physics*. [http://dx.doi.org/10.1063/1.4772998]

Uncovering the neuroanatomical structure of the cerebral cortex of mammals is a major challenge in neuroscience. Results exist only for a limited number of animal species, more notably the cat cortex, which has been divided into 53 cortical areas, linked together by 826 axon fibers. The cat cortico-cortical structure has shown properties of complex networks: a large density of connections causing a short pathlength among nodes, a clustered organization into functional connectivities, and the presence of highly connected areas. One connection architecture that mimics these general aspects of the cat connectivity matrix is a clustered network (or a network of networks), in which each cluster is a scale-free network, presenting one highly connected node, or hub. The hubs, on their way, are strongly connected together (rich-club). Given this peculiar property of the cat cortex network, we have investigated some aspects of the collective dynamics exhibited by a neural network with the same overall structure and where the neuronal dynamics is governed by a model simple enough to allow numerical simulations to be performed with a large number of neurons. We focused, in particular, on the control (suppression) of bursting synchronization when a light pulse is applied to a selected neuron, deactivating it.

I. INTRODUCTION

The cerebral cortex of mammals is a paradigmatic example of a complex network. There is a plethora of phenomena in which the role of the cerebral cortex is vital, like memory, attention, perceptual awareness, thought, language, and consciousness.[1] Hence, the theoretical understanding of the principles of organization and functioning of the cerebral cortex can shed light on the knowledge of many distinct and important subjects in neuroscience.[2] The surface of the cerebral cortex, usually called gray matter, contains basically neurons and their unmyelinated fibers.[3] These neurons are grouped together into functional or morphological units, called *cortical areas*, each of them playing a well-defined role in the processing of information.[4]

From a network perspective of the cerebral cortex the cortical areas form the nodes, linked by fibers (myelinated axons) which chiefly constitute the white matter lying just below the gray matter. These fibers are thus the network connections that link not only adjacent (short-range) cortical areas but also distant (long-range) areas as well. Moreover, the resulting network has been found to be neither exclusively regular nor totally random, but there is some structural complexity underlying these connections.

Detailed information on the anatomic structure of the cerebral cortex network is available only for a limited number of species, particularly the macaque monkey and the cat, the latter having the most complete data set for statistical analyses.[5] The cat cerebral cortex has been divided into 53 cortical areas,[6] interconnected by 826 fibers of axons. From a network point of view, this means a graph with $N = 53$ nodes connected by $L = 826$ links.[6]

There have been performed extensive graph-theoretical analyses of the cat cortical connectivity network and it turns out that it is far more complex than minimal models usually considered in the literature,[7] as random (Erdös-Renyi, ER),

a)Author to whom correspondence should be addressed. Electronic mail: viana@fisica.ufpr.br.

small-world (SW), and scale-free (SF) networks.[8] Basically, the complexity of the cat network is due to the presence of clusters composed by cortical areas with common functional roles.[9] Cortical areas in a given cluster are more densely connected between themselves than with areas of different clusters. This introduces a hierarchical level of complexity that should be reflected in theoretical models of such neuronal networks.[10]

Three major features have been found to govern the organization of the cat cortical connectivity network: (1) a large density of connections causing a very short pathlength among nodes, (2) a clustered organization into functional connectivities, and (3) the presence of highly connected areas, or hubs.[11–13] There have been found areas in the cat network which connect to no less than 60% of other areas. Moreover, these hubs form a dense module in the sense that they are strongly connected among themselves, what has been called a "rich-club" phenomenon.[8] In the cat network, there have been found 11 cortical areas that work as hubs and that such areas have a larger density of links than the network as a whole.

Such analyses have led to a theoretical model that mimics many of the actual features of the cat cortical connectivity: In a lower hierarchical level the network is structured into clusters, where the connections have a power-law connectivity scaling like a scale-free network, which allows the formation of highly connected hubs. In a higher level, such hubs (the "rich-club") are globally connected forming a sub-network with an all-to-all coupling.[14]

It is in fact unknown whether or not the microscopic network of connected neurons in the cat brain satisfies the same connection architecture of the cortical areas, which has been found at the macroscopic level. Most probably at the microscopic level the connections may be even more complex, presenting further hierarchical levels of structure. However, it is nevertheless useful to investigate in what sense the (rather simple) hierarchical structure observed at the macroscopic level could influence the connections among neurons at the microscopic scale.

In this spirit we can assign individual neurons to each node formerly related to a cortical area, and substitute electrical and chemical synapses for the previous axon connections among areas. The distinction among electrical and chemical synapses can be made, within the present model, as follows: Electrical (gap junction) synapses connect neighbor neurons, what amounts to nearest neighbors in a regular lattice; whereas chemical synapses connect distant neurons and are represented by randomly chosen nonlocal shortcuts.

The neuron dynamics generating spiking action potentials is chosen so as to exhibit a desired property to investigate in the context of the present model. A large number of neurons are found to burst, i.e., they repeatedly fire discrete groups (bursts) of spikes, if externally stimulated or due to the interplay of ion currents. A particularly interesting example of bursting cortical neurons are chattering (or fast rhythmic bursting) neurons, that make pyramidal cells able to fire high-frequency bursts of 3 to 5 spikes with a relatively short interburst period.[15]

Since bursting occurs in a longer period than spiking, bursting neurons have to be modelled by systems with a minimal number of variables. Using discrete time systems (maps) for the sake of computational speed, one can model bursting neurons with two-dimensional maps, in which one variable stands for the rapidly spiking action potential, whereas the other acts as a modulating factor and introduces the slower bursting timescale.[16]

Bursting neurons can synchronize due to coupling and it is sometimes undesirable to have such synchronized rhythms, since they may be related to pathologies like essential tremor or Parkinsonian disease. Hence, the suppression of synchronized bursting is of potential interest in the neurosurgery field of deep-brain stimulation.[17] Strategies to suppress synchronized bursting have been proposed in the last years, as the introduction of a time-delayed feedback signal in spatially localized cortical areas (or neurons, in the level of the present model).[18]

The suppression of bursting synchronization may also be obtained through neuron control with light.[19] Recent research has shown the possibility of neuronal inhibition or stimulation with light pulses applied on a targeted neuron, which is adapted with microbial light-sensitive proteins.[20] Such modified neuron is able to produce photosensitive proteins, which releases ions when exposed to light, and it is through the injected current formed by these released ions that the neuronal dynamics can be controlled.

In this paper, we address the problem of how to suppress bursting synchronization in a neuronal network formed by connected clusters. The clusters are described by scale-free networks such that they present hubs of highly connected neurons. These hubs are, on their hand, globally connected (rich-club). The neuronal dynamics is described by a two-dimensional map which enables us to define a bursting phase and the corresponding synchronization. Suppression of bursting synchronization is achieved through external interventions mimicking the application of light to modified neurons.

The rest of the paper is organized as follows: in Sec. II, we present statistical analyses of the cat cortical connectivity that support the use of a rich-club clustered organization in the macroscopic level. Section III outlines the neuron dynamics and the coupled map lattice modeling the neuronal network. It is also defined a bursting phase, as well as the characterization of synchronized states. Section IV deals with the suppression of bursting synchronization through external interventions of the type described above. Our conclusions are left to Sec. VI.

II. CORTICAL CONNECTIVITY OF THE CAT AS A "RICH-CLUB" SYSTEM

A. Weighted adjacency matrix

The cerebral cortex of mammals is innervated by a plethora of corticocortical connections. One of the systems for which these anatomic connections have been extensively studied over the last decades is the cat, for which information from the neuroanatomical literature reporting anatomical tract-tracing experiments has been collected and organized by Scannell *et al.*[5–7] In this dataset the cat cerebral cortex

has been divided into $N = 53$ cortical areas, interconnected by $L = 826$ directed links representing fibers of axons. The overall density of links (i.e., the ratio between the number of links L and the total number of possible directed links connecting N nodes without self-interactions) is thus $\rho_{cat} = L/N(N-1) \approx 0.3$.

The cortical areas are organized into four clusters with common functional roles, namely the visual (V), auditory (A), somatosensory-motor (SM) and frontolimbic (FL), containing 16, 7, 16, and 14 areas, respectively. Out of these 826 connections, a number of 470 are internal (connect areas within the same cluster) and 356 are external (connect areas of different clusters). These cortical areas are identified by anatomical abbreviations that can be found in Table I of Ref. 7.

The corticocortical connectivity of the cat can be summarized by the weighted adjacency matrix $W = (a_{ij})$ depicted in Figure 1, where the 53 cortical areas are identified by their anatomical abbreviations and the weights are assigned according to the axonal density of the fiber projections. Hence, a zero weight ($a_{ij} = 0$) means that the two cortical areas are not connected at all; otherwise, they are connected in three levels of intensity: $a_{ij} = 1, 2, 3$. The four clusters are groups of cortical areas classified by their overall role and form diagonal blocks in the matrix whose elements are internal connections, whereas the elements of off-diagonal blocks stand for the external connections. The diagonal elements a_{ii} are defined to be zero since we do not consider self-interactions of cortical areas. Since the connections are directed (even though two areas may be connected the weights may be different), the adjacency matrix is not expected to be symmetric at all.

A cursory inspection of Fig. 1 reveals that the block-diagonal matrices representing the moduli are quite dense, whereas the off-block-diagonal parts are rather sparse. As a matter of fact, the V, A, SM, and FL clusters have partial link densities of, respectively, 0.58, 0.81, 0.74 and 0.65, whereas the whole network has 0.3 thanks to these sparse off-diagonal blocks.

B. Quantitative measures of clustered structure

As evident from a visual inspection of Fig. 1, a quantitative characterization is needed to establish the clustered structure of the cat network. A thorough analysis of the latter has been made recently, based on the information encoded in the weighted adjacency matrix $W = (a_{ij})$.[11,12] In the following, we outline the basic definitions used and the results of such analysis for the cat network. Further details can be found in Ref. 21, for example.

Let $k_{out}(i) = \sum_{j=1}^{N} a_{ij}$ be the output degree of the ith node ($i = 1, 2, \ldots, N$), i.e., the number of outcoming (efferent) connections projected to other nodes, and $k_{in}(i) = \sum_{j=1}^{N} a_{ji}$ is the input degree, or the number of incoming (afferent)

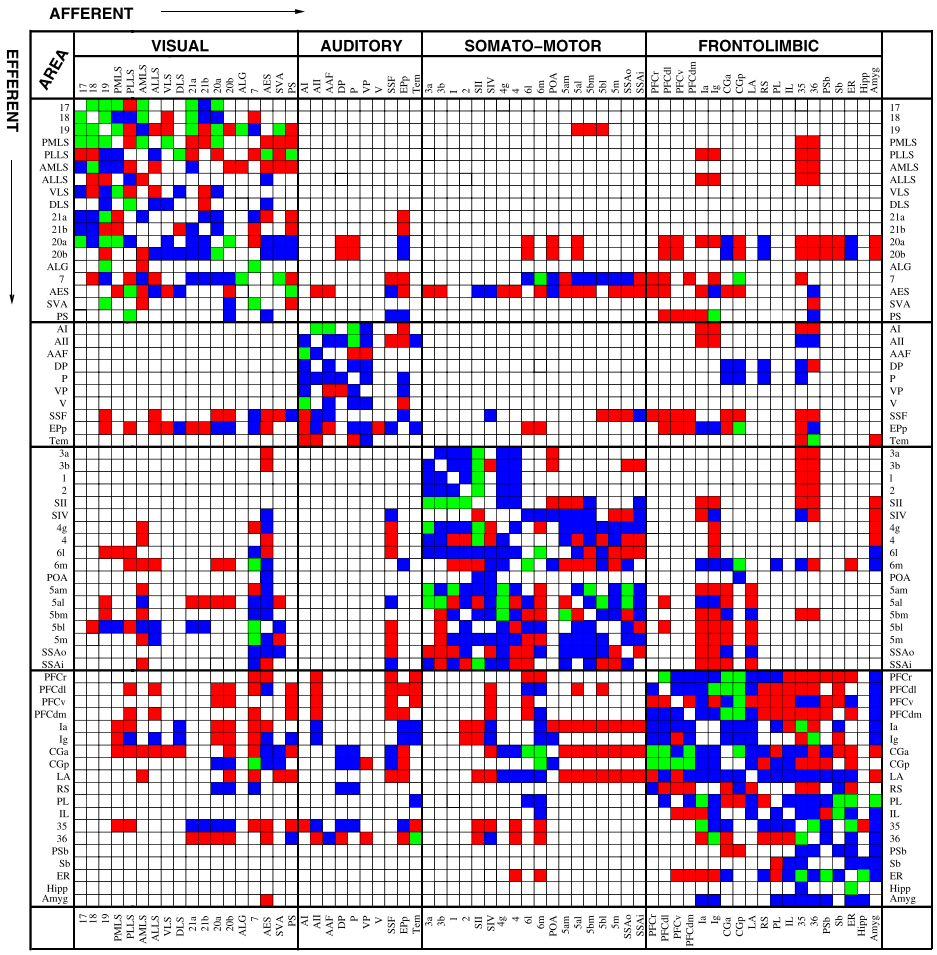

FIG. 1. Matrix representation of the corticocortical connectivity of the cat, according to Table II of Ref. 7. The connections among cortical areas are classified as weak (red), intermediate (blue), and strong (green), with respect to the axonal density of fiber projections.

connections the *i*th node receives from other ones. The degree distribution function $P(k)$ is the probability that a randomly chosen node has a degree k. Closely related is the cumulative degree distribution $P_c(k)$, that is the probability that a randomly chosen node has degree larger or equal to k.

In scale-free networks this degree distribution obeys a power-law $P(k) \sim k^{-\gamma}$, where $\gamma > 0$. In scale-free networks most of the nodes have a small number of connections, whereas a few nodes (called hubs) are highly connected. Scale-free networks can be obtained by the Barabasi-Albert procedure through a sequence of steps starting from an initial lattice with a small number N_0 of nodes.[21] At each step a new node is inserted in the lattice of size N_s, such that it is connected to $l \geq 2$ randomly chosen nodes. The connections occur preferentially with the more connected nodes, thus explaining the production of highly connected hubs. The cat network has been found to possess a cumulative degree distribution somewhat close to that of a scale-free network with the same number of nodes and links, having a degree exponent of 1.5.[12]

Besides the degree distribution, two quantitative measures are commonly used to characterize networks: the average pathlength and the clustering coefficient.[22–28] The distance between two nodes is the length of the shortest path between them in the graph, or the minimal number of links necessary to connect these nodes. The average pathlength ℓ of a network is the average distance between all pairs of nodes. The clustering coefficient C is a measure of degree to which nodes in a network tend to cluster together.

The cat network has been found to have an average pathlength $\ell_{cat} = 0.50$ and a clustering coefficient of $C_{cat} = 1.83$.[12] Random, small-world, and scale-free networks have been generated with the same numbers of nodes ($N = 53$) and directed links ($L = 826$) and appropriate probabilities. The closest average pathlength to the cat network has been found for the small-world network (0.57), whereas the random and scale-free networks have ℓ equal to 0.31 and 0.37, respectively. The clustering coefficient of small-world networks is again very close (1.82) to that found for the cat, and the random (1.70) and scale-free (1.69) not too far from this value.[12]

It seems that the network topology that best suits the cat structure is the small-world one, but this is not the case, however, for two reasons. Small-world networks have no clustered organization, a feature that we found conspicuous in the cat network. Second a small-world network (as the random network as well) has a homogeneous degree distribution, whereas the cat network has a heterogeneous distribution compatible with a scale-free network.[12] In fact, the partial inadequacy of some aspect of small-world, random, or scale-free networks to the cat network structure reveals that the latter is more complex than those minimal models.

C. "Rich-club" clustered network

Based on the previous numerical evidences, a good candidate for a network that mimics the essential features of the cat network would be a clustered network in which each cluster has a scale-free topology. Each of these clusters has a hub, and the question now is how to couple these hubs in a way compatible with the cat network. To answer it, we have to analyze how strongly a hub is coupled with other hubs in comparison with other nodes in the network.

We define the k'-density of connections, denoted as $\rho(k')$, as the internal density of links between nodes with degrees larger than k'. In other words, let $N_{k'}$ be the number of nodes with degree $k \geq k'$ and $L_{k'}$ the number of links among them. The k'-density is thus given by $\rho(k') = L_{k'}/N_{k'}(N_{k'} - 1)$. If we set $k' = 0$, we recover the density of connections of the entire network $\rho(0) = L/N(N-1)$. For the cat network, the k-density of connections has been found to increase monotonically with k.[12]

The relative contribution of hubs in terms of the density of connections can be assessed by comparing the original cat network with surrogate networks (with the same number of links and nodes) where the links have been switched. This washes out the effect of hubs by diluting their effect into the overall network. The k-density of the surrogate networks, called $\rho_{surr}(k)$, is computed for a number of random realization of the surrogates, averages being taken. If the k-density $\rho(k)$ grows with k faster than $\rho_{surr}(k)$, it means that the hubs are more densely connected than the other nodes and form a dense module (the "rich-club").

The k-density $\rho(k)$, for the cat network, increases faster than $\rho_{surr}(k)$ for the surrogates after $k = 15$, the largest difference being observed for a degree $k = 23$.[12] In the latter case, the "rich-club" has out of 11 members, distributed among the clusters as follows: 3 hubs for the V cluster, one hub for A, two for SM, and 5 for FL. Hence, the hubs for the cat network form a strongly connected network.

This body of quantitative evidence for the cat network supports our using of a clustered network in which each cluster has a scale-free topology and the hubs are coupled through global (all-to-all) connections. This kind of network is schematically depicted in Fig. 2: At the lowest hierarchical level the clusters are scale-free sub-networks and, at the highest level, there is a densely interconnected overlap of the modules through a global coupling of the corresponding hubs.

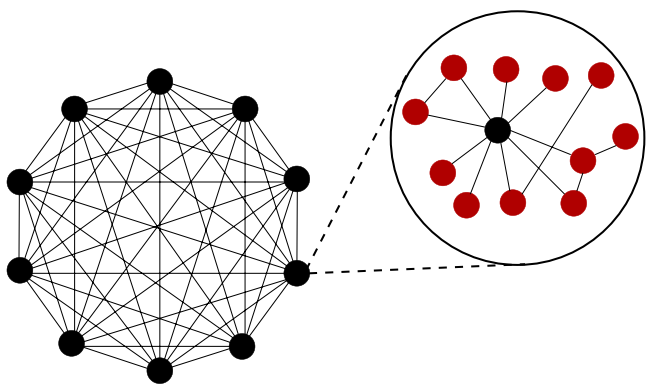

FIG. 2. Schematic hierarchical organization of a rich-club clustered network.

III. "RICH-CLUB" MODEL FOR THE NEURONAL NETWORK

A. Neuronal dynamics

Many neurons do not only spike but also burst, i.e., they emit rapid sequences of spikes separated by comparatively quiescent periods. For such neurons, there are two time scales: a fast timescale for the spiking activity and a slow timescale for the bursting itself. Discrete-time models of bursting neurons thus require two variables: x which stands for transmembrane voltage, as in integrate-and-fire models, which describes the fast spiking dynamics, and y, called a recovery or adaptation variable, which takes into account the slower bursting dynamics.

Denoting by n the time, a family of two-dimensional map-based models of this kind is described by the following equations:

$$x_{n+1} = F(x_n, y_n), \tag{1}$$

$$y_{n+1} = y_n + \varepsilon(y_n - \tilde{\sigma}x_n - \tilde{\beta}), \tag{2}$$

where F is a function that embodies the sub-threshold behavior of the membrane voltage, and includes a threshold and reset mechanism to generate spikes. The separation between fast and slow timescales is provided by keeping the parameter ε small enough, in such a way that variations of y are slower than those of x. Accordingly $\sigma = \varepsilon\tilde{\sigma}$ and $\beta = \varepsilon\tilde{\beta}$ are small parameters for the slow dynamics, which incorporate the action of synaptic inputs and also the action of some intrinsic currents that are not explicitly captured by model.[29,30]

There have been proposed other maps that display a two-scale (spiking-bursting) neuronal dynamics: Chialvo,[31] Copelli *et al.*,[32] and Izhikevich,[33] among others. Rulkov has proposed a model that fits the general form above, and reads

$$x_{n+1} = \frac{\alpha}{1 + (x_n)^2} + y_n, \tag{3}$$

$$y_{n+1} = y_n - \sigma x_n - \beta, \tag{4}$$

where $F(x, y) = \alpha/(1 + x^2) + y$ is a smooth function that includes both a chaotic spiking dynamics (for values of α within the range [4.1, 4.4]) and also a threshold-and-reset mechanism, which is incorporated through a piecewise function in similar models.[31] We choose here α to be our variable parameter for numerical simulations, whereas the slow dynamics will have small parameters $\sigma = \beta = 0.001$ kept constant.

A typical output generated by this map is illustrated in Fig. 3, obtained for $\alpha = 4.1$. The fast variable exhibits a sequence of bursts, each being a rapid sequence of spikes succeeded by a quiescent period [Fig. 3(a)]. The onset of a burst coincides with a local maximum of the slow variable [Fig. 3(b)]. Moreover, the oscillation amplitude for the slow variable is only ~6% of the corresponding variation of the fast variable. The dynamical mechanism underlying the appearance of bursts in the Rulkov map can be inferred from a one-dimensional approximation. Since y_n is always a small variable (in comparison with x_n), we can approximate it by a constant γ and analyze the resulting one-dimensional map $x_{n+1} = \alpha/(1 + x_n^2) + \gamma$. This map has generally three fixed points $x^*_{1,2,3}$ such that the first two undergo a saddle-node bifurcation as γ approaches a critical value γ^*.[29] When $\gamma \gtrsim \gamma^*$, the fixed points $x^*_{1,2}$ disappear and a narrow channel forms between the map function and the 45°-line such that the fast variable displays chaotic oscillations corresponding to the spikes within a given burst. The end of the burst, on the other hand, is due to an external crisis of the chaotic attractor.

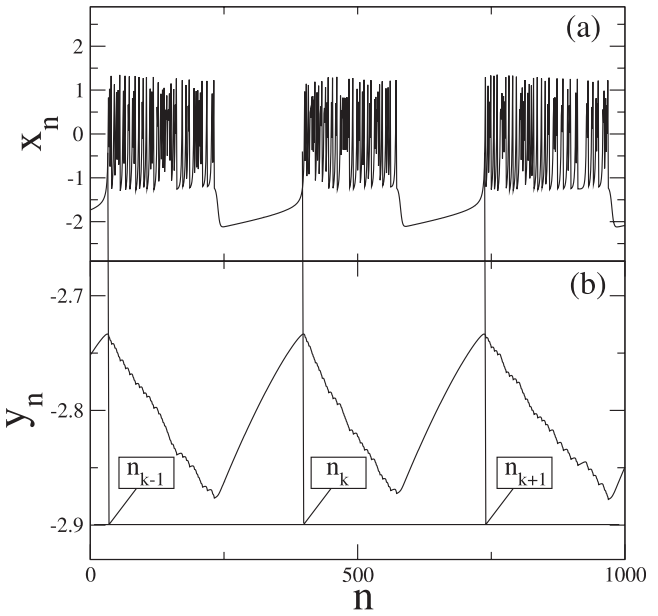

FIG. 3. Time evolution of the (a) fast and (b) slow variables in the Rulkov map (3) and (4) for $\alpha = 4.1$, $\sigma = \beta = 0.001$, showing the times sampled to define a bursting phase.

The coincidence between the beginning of a burst and a local maximum of the slow variable enables us to define a geometric phase for the bursting dynamics. Let n_k be the times at which y_n has a local maximum [Fig. 3(b)]. The duration of the chaotic burst, $n_{k+1} - n_k$, depends on the variable x_n and fluctuates in an irregular fashion when x_n undergoes a chaotic evolution. The bursting phase is thus defined as[34]

$$\varphi(n) = 2\pi k + 2\pi\frac{n - n_k}{n_{k+1} - n_k}, \tag{5}$$

such that its values go from 0 to 2π as n evolves from n_k to n_{k+1}.

B. Scale-free network

In the neural network model to be studied in this work, we have a clustered "rich-club" structure: The clusters are scale-free networks possessing hubs, or highly connected nodes. These "rich" nodes are coupled together globally, i.e., each hub interacts with the mean-field produced by all other hubs. Let us briefly describe how this structure is generated for numerical simulation purposes.

We consider S clusters, each of them with N neurons. The fast and slow variables for a neuron in a given cluster are denoted as $x_n(i, \ell)$ and $y(i, \ell)$, respectively, where $i = 1$,

2,…, N and $\ell = 1, 2, \ldots S$. The dynamics of the coupled neurons described by the Rulkov map (3) and (4) is governed by the following network equations:

$$x_{n+1}(i,\ell) = \frac{\alpha(i,\ell)}{1 + x_n^2(i,\ell)} + y_n(i,\ell) + \mathcal{C}_n(i,\ell), \tag{6}$$

$$y_{n+1}(i,\ell) = y_n(i,\ell) - \sigma x_n(i,\ell) - \beta. \tag{7}$$

Note that the small parameters σ and β take on the same value for all neurons, whereas the parameter α was allowed to have slightly different values for each neuron, randomly chosen with uniform probability within the interval [4.1, 4.4]. The reason for this choice is that we take the neurons as slightly different from each other. The range of α is limited, since we want to keep all neurons in the bursting regime. On the other hand, modifying the slow variables does not show results as noticeable than varying α.

The coupling term is applied to the fast variable only because the synaptic connection with other neurons introduces external currents that directly influence the membrane potential, whose spiking dynamics is modelled by the x variable. In each cluster, the corresponding sub-network has a scale-free connectivity represented by the coupling term $\mathcal{C}_n(i,\ell)$ given by

$$\mathcal{C}_n(i,\ell) = \frac{\varepsilon}{k(i,\ell)} \sum_{j \in I, j \neq i} x_n(j,\ell), \tag{8}$$

where $\varepsilon > 0$ is an overall coupling strength and we assume that each neuron i belonging to the cluster ℓ is coupled with a set I comprising $k(i,\ell)$ other neurons from the same cluster. The coupling proposed is a first order approximation for an excitatory chemical coupling.

We build the scale-free network for each cluster $\ell = 1, 2, \ldots S$ according to the Bárabasi-Albert procedure, by means of a sequence of steps $s = 0, 1, 2, \cdots s_{max}$ and starting from an initial network with $N_0 = 11$ nodes.[21] At each step s a new site is inserted in the network of size N_s, such that it is connected to $L \geq 2$ randomly chosen sites. The connections are set preferentially with the already more connected nodes, what can be accomplished by using a different probability for each node $P_s(i,\ell) = k_s(i,\ell)/N_s$, where $k_s(i,\ell)$ is the number of connections *per* node at the step s. The process is repeated until we achieve a desired network size N. After a number s_{max} of steps we have $k(i,\ell)$ connections *per* node, corresponding to a probability $P(i,\ell) = k(i,\ell)/N$.

Figure 4 depicts a histogram for the number of nodes with connectivity k in each cluster, obtained through this procedure for $N = 230$ nodes. The numerical approximation to the (non-normalized) probability is shown to display the scale-free signature of a power-law scaling $k^{-\varpi}$ with a slope $\varpi = 2.08$. In each cluster we have, by construction, a single most connected node which we call the cluster hub. For the network degree distribution of Fig. 4 the hub has 30 connections, whereas most of the other nodes have five or less connections.

Let us denote by $\hat{x}(\ell)$ the fast variable of the most connected node of the ℓth cluster. In the clustered "rich-club" structure, the hubs are globally connected to each other with a different coupling strength ε_h. Hence, the governing equation for these "upper class" neurons is

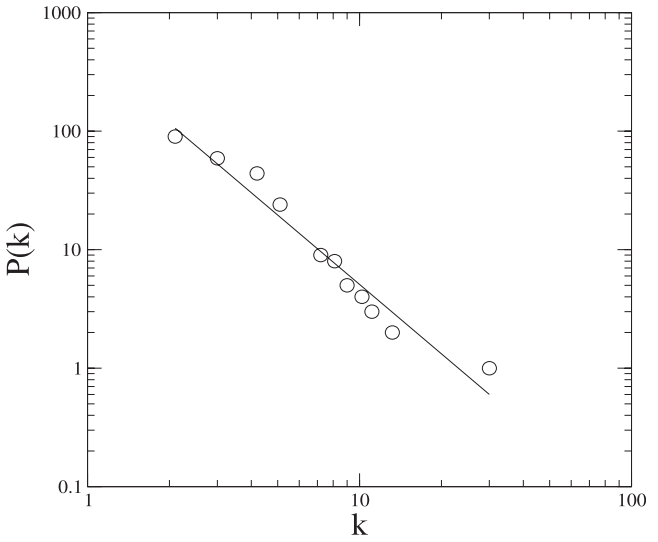

FIG. 4. Probability distribution for the connectivity of the scale-free network representing a cluster with $N = 230$ nodes. The solid line is a least-square fit with slope − 2.08.

$$\hat{x}_{n+1}(\ell) = \frac{\alpha(\ell)}{1 + x_n^2(\ell)} + y_n(\ell) + \frac{\varepsilon_h}{S} \sum_{m=1}^{S} \hat{x}_n(m), \tag{9}$$

where we have coupled only the fast variables of the hubs, just like we did for the clusters themselves. The neural network model we have described is defined in a graph-theoretical sense. Hence, it has no need of boundary conditions. However, initial conditions $(x_0(i,\ell), y_0(i,\ell))$ must be defined for all NS neurons, and we have chosen randomly those values.

IV. BURSTING SYNCHRONIZATION

There are many definitions of synchronized behavior in the neuroscientific literature. Perhaps the strongest form of synchronization among bursting neurons would be complete synchronization, whereby different neurons in a network have the same variables for all times. For a cluster with M such neurons, we would have $(x_n(1), y_n(1)) = (x_n(2), y_n(2)) = \cdots = (x_n(M), y_n(M))$. This form of synchronization is, however, too strong to fit the requirements posed by real neural networks. For example, it is unlikely that the coupled neurons are identical, a necessary condition for the occurrence of completely synchronized states.

A milder form of synchronization is spiking synchronization, by which the coupled neurons are required to spike at the same time during the active phase of their bursting. An even milder form is bursting synchronization, in which only the bursting time must be the same for the coupled neurons, regardless of the subsequent development of their active phases. It is obvious that spiking synchronization implies bursting synchronization, but the opposite is not necessarily true. We can have two neurons beginning their bursts at the same time but with a subsequent out-of-phase spiking behavior during their active phases.[34]

1. Order parameter

A quantitative way to characterize bursting synchronization is through the corresponding bursting phases, as defined in Eq. (5). A given subset with M neurons is said to exhibit bursting synchronization if their phases coincide: $\varphi_n(1) = \varphi_n(2) = \cdots = \varphi_n(M)$ for all times n. We have purposely chosen slightly mismatched parameters for each neuron so as to avoid the undesired possibility of complete synchronization and allowing the study of the comparatively weaker bursting synchronization. Bursting synchronization may occur via synaptic coupling or through a common injected inputs, as external currents. In this work, we shall deal with the former case.

A diagnostic of bursting synchronization is provided by the Kuramoto's order parameter z.[35] Let M be the number of neurons in a given assembly: If a single cluster is considered then $M = N$, whereas $M = NS$ for the entire network. Smaller assemblies can possibly be chosen, however, since it is unlikely that, on biological grounds, the entire brain becomes synchronized whatsoever. An example is the rich-club itself, formed by the well-connected hubs, for which $M = S$. In any of these cases, the complex order parameter is defined as

$$z_n = R_n e^{i\Phi_n} \equiv \frac{1}{M}\sum_{j=1}^{M} e^{i\varphi_n(j)}, \tag{10}$$

where R_n and Φ_n are the amplitude and angle, respectively, of a centroid phase vector.

In a globally synchronized situation all the bursting phases coincide and thus the terms in (10) add coherently and, after divided by M, the magnitude asymptotes the unity. If, on the other hand, we have such an extreme nonsynchronized case that the bursting phases $\phi_n(j)$ are totally uncorrelated, their contribution to the summation in Eq. (10) is small and actually vanishes for $N \to \infty$. Since the order magnitude amplitude R_n typically oscillates with time it is better to work with its time-average $\overline{R} = \frac{1}{T}\sum_{n=1}^{T} R_n$, where T is chosen to be a time window after the initial transient dies off. In practice, a fairly good bursting synchronized regime is achieved when $\overline{R} > 0.90$.

The connection architecture used in our model has two variable parameters: the coupling strength within a cluster ε and the coupling strength among the hubs ε_h (rich-club). In Fig. 5, we show (in colorscale) the time-averaged order

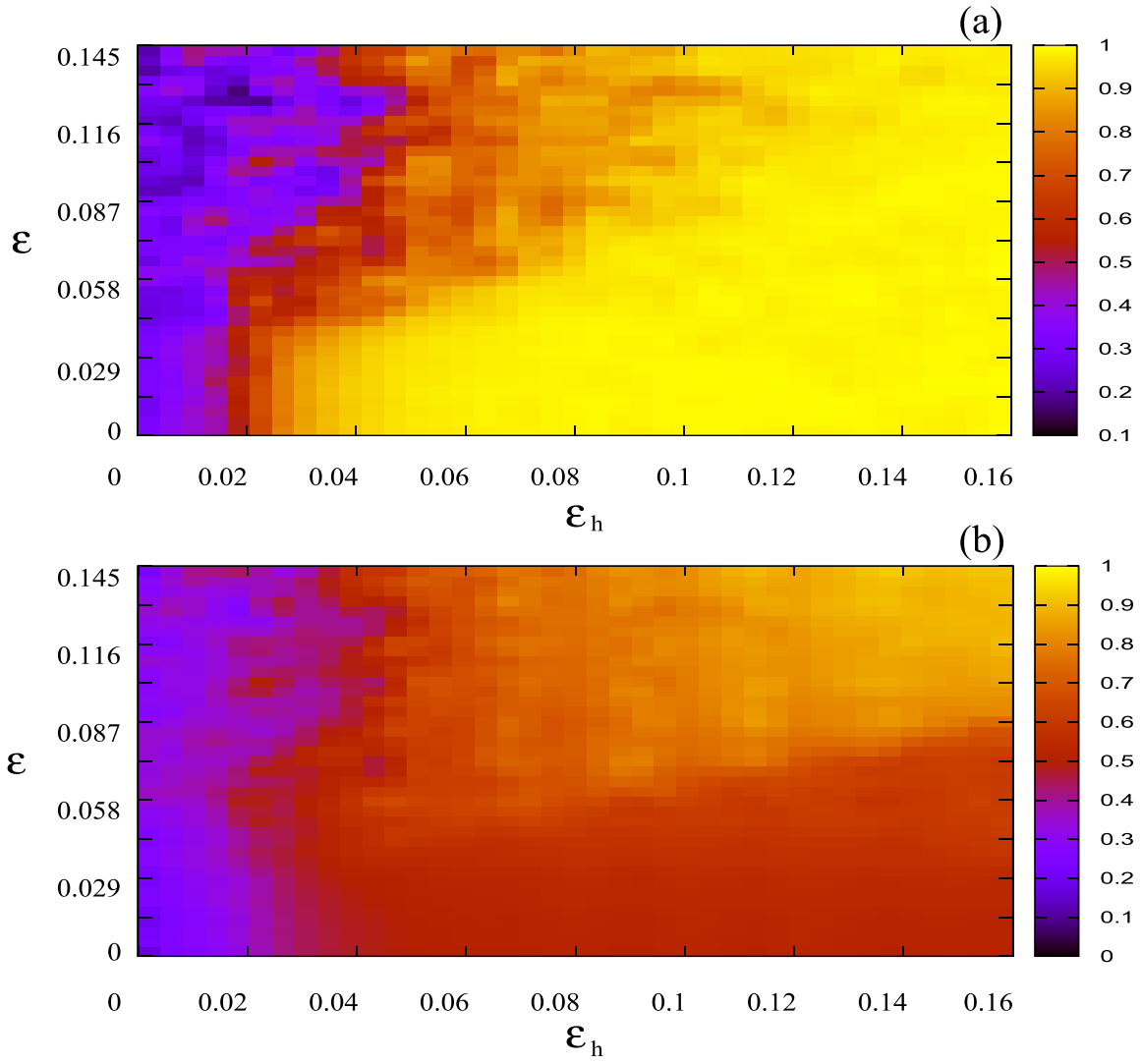

FIG. 5. Time-averaged order parameter magnitude as a function of the coupling strength of the clusters and of the rich-club for an assembly consisting of (a) only the hubs (the rich-club itself); (b) the entire network. We consider $S = 10$ scale-free clusters with $N = 253$ nodes each.

parameter magnitude *versus* both coupling strengths. If we analyze only the rich-club of globally connected $M = S$ hubs [Fig. 5(a)], we observe that it is relatively easy to achieve complete bursting synchronization by increasing the rich-club strength to a high enough value, which is $\varepsilon_h \sim 0.03$ if the neurons in each cluster are themselves uncoupled. It is quite noteworthy that this value increases as we consider larger values of ε, since this suggests that the coupling of neurons within the clusters affects the synchronization of the rich-club members.

This is only at the first view counterintuitive since, as the neurons couple within the clusters, the clusters themselves may synchronize at different values, and so the corresponding hubs. This observation is confirmed by Fig. 5(b), in which the order parameter of the entire network (for which $M = NS$) is considered. For a large number of values of ε_h yielding synchronization within the rich-club, we have a poorly synchronized network as a whole, i.e., the clusters remain non-synchronized even though their hubs are synchronized.

In Fig. 6(a), we plot the $\overline{R}$ as a function of the coupling strength ε in a network with $S = 10$ and $N = 230$, for each cluster (solid black lines) and for the entire network (red line). The rich-club coupling ε_h was kept constant. For small values of the coupling strength ε the values of $\overline{R}$ are small, yet nonzero. A standard explanation for this fact would be the chance correlations introduced by our using of a finite (and small) number of neurons N. However, recently it has been proposed that this fact can be due to the existence of neurons evolving around periodic stable orbits of their dynamics, what yields an approximately constant local mean field, a phenomenon called *collective almost synchronization*, a universal phenomenon appearing in complex networks for small coupling strengths.[36] Moreover, for small coupling we see that the clusters synchronize relatively fast compared with the entire network. We can identify a region I ($0 < \varepsilon \lesssim 0.075$) below the synchronization threshold of 0.90 for both the clusters and the network. This means that the clusters synchronize at different levels, what decreases the overall effect in the network.

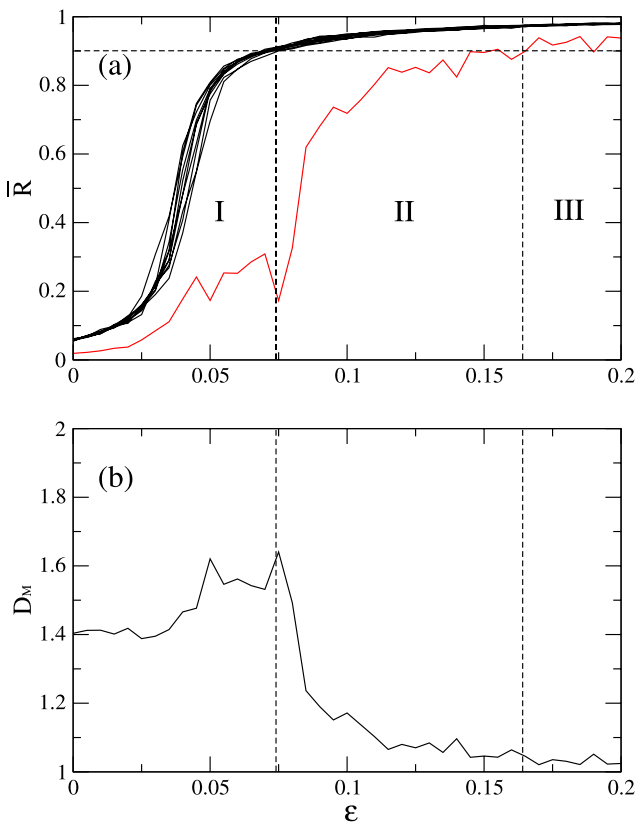

FIG. 6. (a) Time-averaged order parameter magnitude as a function of the coupling strength ε for each cluster (solid black lines) and for the entire network (red line). (b) The same variation for the dynamical modularity. We consider a clustered network with $S = 10$, $N = 230$, and $\varepsilon_h = 0.16$.

For intermediate couplings the clusters remain synchronized and the network begins to synchronize as well, indicating that the values at which the individual clusters synchronize become more and more close to each other. This defines a region II ($0.075 \lesssim \varepsilon \lesssim 0.170$), above the 0.90 threshold for the clusters and below it for the network. Increasing the coupling strength further turns the entire network as synchronized as the clusters themselves, what defines a region III ($\varepsilon \gtrsim 0.170$), above the threshold for both clusters and network, that constitutes global bursting synchronization, whereas region II indicates only modular bursting synchronization.

2. Dynamical modularity

This discrepancy between the synchronized behavior of the rich-club and of the clusters can be also described by other means. Clustered behavior can be investigated by means of the so-called dynamical modularity, which compares the degree of synchronization within clusters with the average dynamical correlation among the clusters. The average self-correlation of a given cluster, denoted by $R_{\ell\ell}$, is computed by using the order parameter magnitude for the cluster ℓ only, whereas the average intercluster cross-correlation $R_{\ell m}$ is obtained from the order parameter magnitude computed by taking into account the clusters ℓ and m. If the entire network has S clusters, the dynamical modularity D_M is defined as[14]

$$D_M = \frac{(1/S)\sum_{\ell}^{S} \overline{R_{\ell\ell}}}{(1/S(S-1))\sum_{\ell}^{S}\sum_{m\neq\ell}^{S} \overline{R_{\ell m}}}. \qquad (11)$$

When the network presents a behavior consistent with clustered behavior, D_M presents values above unity and bursting synchronization of assemblies or moduli is possible. Accordingly, this behavior has been called modular synchronization. On the other hand, if D_M is near (or less than the) unity then the network behavior is not consistent with a clustered structure and the bursting synchronization of the whole network is more important than the behavior of its clusters.

In Fig. 6(b) we plot D_M against ε for the same network considered in Fig. 6(a), taking into account the same regions of similar qualitative behavior, with respect to bursting synchronization. In region I (non-synchronized behavior) D_M is clearly above the unity, having values between 1.4 and 1.6, what indicates modular behavior. Region II, where the

clusters are synchronized but the network is not, presents a decreasing D_M, as expected. In fact, the difference between the order parameter of the clusters and of the network itself is a consequence of the modular behavior: The clusters behave in distinct ways from the entire network. In region III, where both the clusters and the network are synchronized, the modular behavior of the network is less evident, and hence $D_M \approx 1$.

3. Mean field

Given that it may happen that the clusters synchronize at different values, what hinders synchronization of the entire network, we could ask how different clusters behave in such circumstances. To answer this question, it is useful to compute the mean field for a cluster $\ell = 1, 2, \ldots S$ as a function of time: $\mathcal{M}_n(\ell) = (1/N)\sum_{i=1}^{N} x_n(i,\ell)$. If the entire network is considered, then we compute the corresponding total mean field $\mathcal{M}_{Tn} = (1/NS)\sum_{i=1}^{N}\sum_{\ell=1}^{S} x_n(i,\ell)$.

From the computational point of view, the mean field is useful since, whenever there is bursting synchronization within the cluster (or the network), the corresponding mean field exhibits large-amplitude oscillations.[17] On the other hand, if there is no synchronization the mean field presents small-amplitude noisy oscillations. From the neuroscientific point of view, the mean field has also its merits: It has been observed that pathologically large amplitude brain activity appears due to a synchronized bursting of a large number of neurons in specific regions of the brain.[37,38] These synchronized states are thought to play a key role in some conditions like Parkinson's disease and essential tremor.[39,40] The mean field, appearing to the existence of collective synchronized bursting, is thus related (in a probably very complicated manner) to the macroscopic tremors observed in clinical studies.[41] Indeed, techniques of deep-brain stimulation have been successful on reducing the amplitude of these tremors, what has encouraged a number of theoretical studies relating this procedure to the suppression of bursting synchronization.[42]

The time evolution of the mean field for two clusters and for the entire network is depicted in Fig. 7 for coupling strengths belonging to the three qualitatively different classes of behavior represented in Fig. 6. For small coupling strength ($\varepsilon = 0.025$, belonging to region I of sub-threshold behavior), there is indeed no evidence for synchronization for both the clusters and the network, since the mean field has small fluctuations. For a coupling strength in the region II ($\varepsilon = 0.085$, sub-threshold for the network only), the clusters exhibit synchronized behavior (large amplitude oscillations) in an independent way: The mean field oscillations are out of phase. As a matter of fact, the mean field of the network presents oscillations of much smaller amplitude and rather irregular, whereas the cluster oscillations are clearly periodic. Finally, for region III ($\varepsilon = 0.2$, supra-threshold global behavior) the mean field oscillates almost in unison with the clusters, illustrating the occurrence of global bursting synchronization.

V. SUPPRESSION OF BURSTING SYNCHRONIZATION

The encouraging results of deep-brain stimulation in the reduction or suppression of abnormal brain rhythms (often leading to pathological tremor and other conditions) suggest that it is worthwhile to pursue the suppression of bursting synchronization, once it appears in specific regions of the brain, through some means. In previous works, we have considered two methods to do so by using external interventions: In the direct current injection, a weak ac-signal with carefully chosen amplitude and frequency is inserted on a network presenting global synchronized behavior.[34] Such studies have been performed with some types of coupling schemes: global, scale-free, small-world, etc.[43] Other kind of control consists on a time-delayed feedback signal which records the network mean field at both actual and previous times, adjusting the control strength by the difference between such mean fields (time-delayed feedback).[17,44] The latter procedure has been also applied to scale-free networks.[18] We have proved that this method is also effective in clustered networks where the neurons can be randomly coupled to neurons belonging or not to the same cluster, although with different probabilities.[45]

In this work we pursue a third possibility of suppressing bursting synchronization, once it occurs in a scale-free clustered network of the rich-club type. Instead of applying an electrical signal on some neuron, we deactivate the neuron through the use of an external perturbation. In particular, we consider a perturbation similar to an optical neuronal

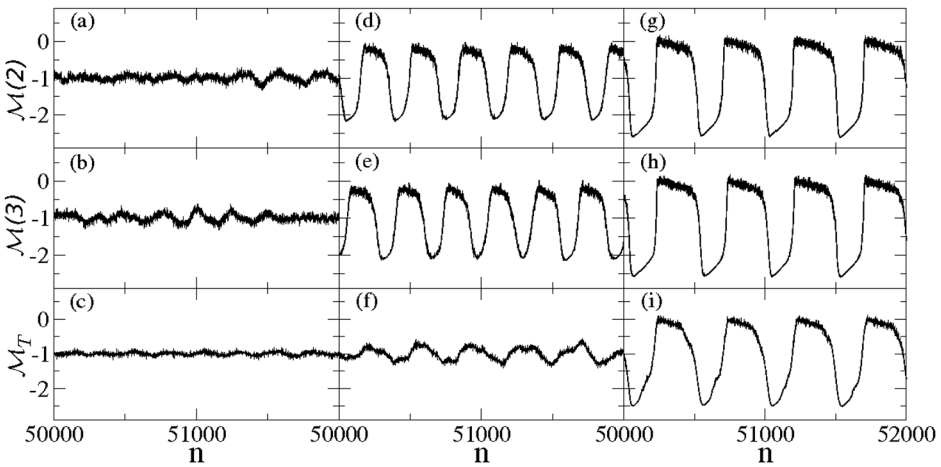

FIG. 7. Time evolution of the mean field time evolution of two clusters ($\mathcal{M}(2)$ and $\mathcal{M}(3)$) and the entire network $\mathcal{M}_T$ for $\varepsilon =$ 0.025 [(a), (b), and (c)], 0.085 [(d), (e), and (f)], and 0.2 [(g), (h), and (i)].

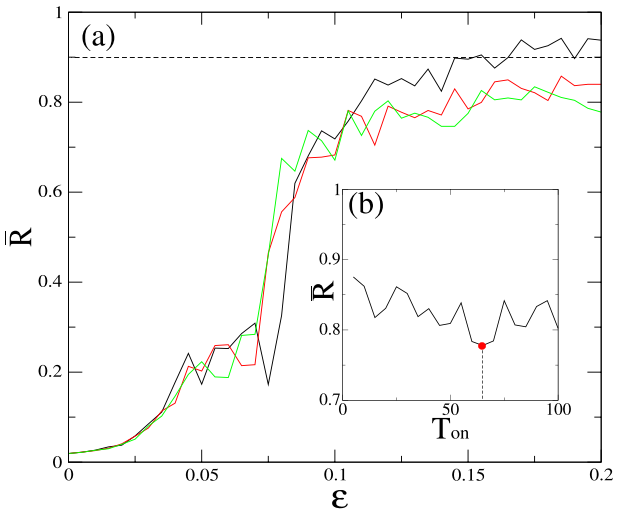

FIG. 8. (a) Time-averaged global order parameter as a function of coupling strength for no external perturbation (black), a constant perturbation (red), and a pulsed perturbation (green) with $T_{on} = 65$ and $T_{off} = 100$. The remaining parameters are the same as in Fig. 6. (b) $\overline{R}$ versus T_{on} for $T_{off} = 100$ and other parameters have been kept unchanged. The red circle corresponds to the value used in (a).

inhibition, i.e., a neuron is deactivated by a light beam of a specific frequency. Whenever this neuron receives the light pulse it is forbidden to spike, what amounts to a low-pass filter applied to the fast dynamics when the control is on.[20] There has been experimentally verified that pulses of yellow light can silence the spiking of a neuron in a reversible way, for the spiking resumes activities when the light stimulation ceases.[19]

We consider a perturbation consisting of light pulses applied to a specific neuron hub (from one of the clusters) using two protocols: (i) a constantly applied pulse deactivating a selected neuron and (ii) an alternating on-off pulse, such that during a time T_{on} the selected neuron is deactivated by a light pulse, followed by a time T_{off} during which no perturbation is applied whatsoever. The effect of such protocols on the suppression of bursting synchronization is illustrated by Fig. 8(a), where the time-average (global) order parameter magnitude is plotted against ε without any control (black line), with constant application [protocol (i)] (red line), and with pulsed application [protocol (ii)] (green line), with $T_{on} = 45$ and $T_{off} = 100$.

We have considered, in a rather arbitrary but usual way, the network to be bursting-synchronized whenever the value of $\overline{R}$ exceeds 0.90 (indicated in Fig. 8(a) by a dashed line). According to this convention, the uncontrolled network becomes synchronized (with respect to their bursting phases) for $\varepsilon \gtrsim 0.15$. Both protocols of control are shown here to be able to suppress synchronization for all values of ε considered in our numerical simulations. It is worth noticing that the suppression effects are only effective for $\varepsilon \gtrsim 0.10$, and that both protocols have comparable efficiency when they are intended to work. Hence, it is not necessary to apply the light pulses (or other deactivating procedure) constantly in time to achieve suppression of synchronization.

As a consequence, protocol (ii) seems to be more energy-saving than protocol (i). In particular, we can seek for an optimal choice of the on-off periods for pulsed application. In Fig. 8(b) we plot the time-averaged order parameter magnitude for different periods of application T_{on}, keeping a fixed value of the inactivity $T_{off} = 100$. The lowest value of $\overline{R}$, meaning here the most non-synchronized behavior, is achieved for $T_{on} = 65$ (indicated as a red circle in Fig. 8(b)), what suggests a ratio of $T_{on}/T_{off} = 0.65$ for this kind of protocol.

When considering an external controlling intervention on a neural network exhibiting synchronized bursting, we have to keep in mind the need to suppress synchronized bursting, not the bursting itself. Hence, it is always important to ask: Is our control weak enough so as not to destroy bursting activity? For this analysis, we plot in Figs. 9(a) and 9(c) the spiking variable (the action potential) of a selected hub without and with perturbation, respectively, considering a pulsed application [protocol (ii)] with $T_{on}/T_{off} = 0.65$. We see in Figs. 9(b) and 9(d) that the subnetwork mean field of the perturbated hub does not have relevant modifications

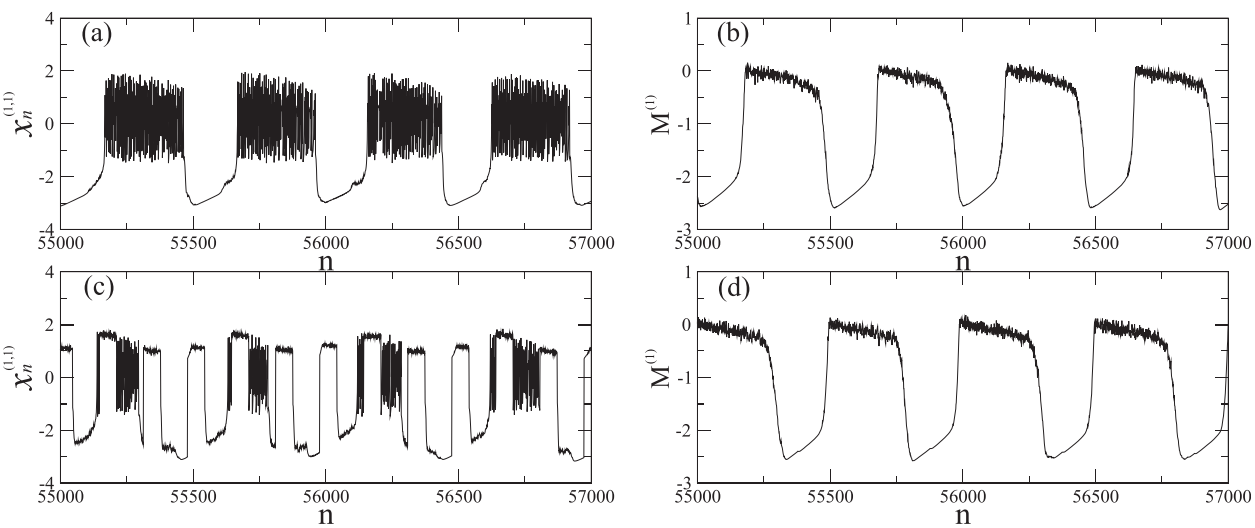

FIG. 9. Time evolution of the spiking (fast) variable for one hub without (a) and with (c) a pulsed perturbation with $T_{on}/T_{off} = 0.65$. (b) and (d) are the mean fields corresponding to (a) and (c), respectively.

compared with the normal dynamics. Then, this perturbation is not able to destroy the natural behavior of the subnetwork, even though the hub itself displays a significative modification of its spiking-bursting activity.

An important question which arises in this investigation is to what neuron we should apply the control to obtain an enhanced performance? This is equivalent to maximizing the controllability of a neural network by selecting appropriate neurons to act upon, and designing suitable control protocols. This task has been pursued by Tang and collaborators, who developed a method to minimize the eigenratio and the maximum imaginary part of an extended connection matrix, i.e., to convert the problem into a constrained optimization problem (COP).[46]

VI. CONCLUSIONS

In this work, we consider a neural network model of clustered scale-free networks tailored to mimic the cortico-cortical connectivity of the cat. An analysis based on topological and metric properties of the latter matrix suggests that a connection architecture that matches some basic properties of the cat is a "rich-club" of clusters, each of them exhibiting a scale-free connectivity property and with a well-connected hub. These hubs, on their hand, are strongly connected to each other, and we have chosen a global (all-to-all) coupling to simulate this effect.

The main problem addressed in this paper is how to suppress bursting synchronization in a network of Rulkov neurons connected in a clustered scale-free network of the "rich-club" type. Among the various external controlling interventions we have chosen to deactivate a selected neuron, what is experimentally feasible applying light pulses. One advantage of the latter procedure is that it is non-invasive, unlike low-frequency current injection, as used in deep-brain stimulation techniques. Another is that the intervention using light pulses is reversible.

We find that this controlling procedure is effective to suppress bursting synchronization even if the light deactivation is performed on a single neuron. This remarkable result is a consequence of the clustered structure of our network model, in which the hubs are so strongly connected that any intervention performed on a given hub is rapidly spread out the network, influencing the clusters. We are considering also control interventions caused by low-frequency current injection and time-delayed feedback signals. However, the general trends presented in this work seem to appear also when these invasive techniques are applied.

A still open problem consists in choosing a control protocol that is optimal in the sense that it has the better possible effect using a minimum amount of energy, i.e., minimizing the value of the control strength. A possible way to solve this problem is to use the constrained evolutionary method for detecting the best controlling cortical regions, according to Ref. 46. Once such optimization procedures are implemented, better control protocols, combined with a more thorough understanding of the cortical networks, could be used to evaluate results of *in vivo* procedures to control undesired and pathological abnormal rhythms associated with many forms of synchronization.

ACKNOWLEDGMENTS

This work was made possible through partial financial support from the following Brazilian research agencies: CNPq, CAPES, and Fundação Araucária. J.K. was supported by the Federal Ministry of Education and Research, Germany (BCCN2, Grant No. 01GQ1001A) and the Deutsche Forschungsgemeinschaft, research group FOR 868 (Contract No. KU837/23-2). We acknowledge G. Zamora-López for useful discussions.

[1]G. Buzsaki, *Rhythms of the Brain* (Oxford University Press, 2006).
[2]C. C. Hilgetag and M. Kaiser, "Organization and function of complex cortical networks," in *Lectures in Supercomputational Neuroscience (Dynamics in Complex Brain Networks)*, edited by P. B. Graben, C. Zhou, M. Thiel, and J. Kurths (Springer, Berlin, 2008).
[3]E. R. Kandel, J. H. Schwartz, and T. M. Jessell, *Principles of Neural Science*, 4th ed. (McGraw-Hill, 2000).
[4]P. Rakic, Science **241**, 170 (1988).
[5]J. W. Scannell and M. P. Young, Curr. Biol. **3**, 191 (1993).
[6]J. W. Scannell, C. Blakemore, and M. P. Young, J. Neurosci. **15**, 1463 (1995).
[7]J. W. Scannell, G. A. P. C. Burns, C. C. Hilgetag, M. A. O'Neil, and M. P. Young, Cereb. Cortex **9**, 277–299 (1999).
[8]G. Zamora-López, C. Zhou, and J. Kurths, Front. Neurosci. **5**, 83 (2011).
[9]C. C. Hilgetag, G. A. Burns, M. O'Neill, J. W. Scannell, and M. P. Young, Philos. Trans. R. Soc. London, Ser. B **355**, 91 (2000).
[10]C. C. Hilgetag and M. Kaiser, Neuroinformatics **2**, 353 (2004).
[11]G. Zamora-López, C. Zhou, and J. Kurths, Chaos **19**, 015117 (2009).
[12]G. Zamora-López, C. Zhou, and J. Kurths, Front. Neuroinformatics **4**, 1 (2010).
[13]L. Zemanova, C. Zhou, and J. Kurths, Physica D **224**, 202 (2006).
[14]J. Gómez-Gardeñes, G. Zamora-López, Y. Moreno, and A. Arenas, PLoS ONE **5**, e12313 (2010).
[15]C. M. Gray and D. A. McCormick, Science **274**, 109 (1996).
[16]B. Ibarz, J. M. Casado, and M. A. F. Sanjuán, Phys. Rep. **501**, 1 (2011).
[17]M. G. Rosenblum and A. S. Pikowsky, Phys. Rev. E **70**, 041904 (2004).
[18]C. A. S. Batista, S. R. Lopes, R. L. Viana, and A. M. Batista, Neural Networks **23**, 114 (2010).
[19]X. Han and E. S. Boyden, PLoS ONE **2**, e299 (2007).
[20]F. Zhang, A. M. Aravanis, A. Adamantidis, L. Lecea, and K. Deisseroth, Nat. Rev. Neurosci. **8**, 577 (2007).
[21]R. Albert and A.-L. Barabási, Rev. Mod. Phys. **74**, 47 (2002).
[22]D. J. Watts, *Small Worlds* (Princeton University Press, Princeton, 2000).
[23]P. Erdös and A. Rényi, Publ. Math. **6**, 290 (1959).
[24]D. J. Watts and S. H. Strogatz, Nature **393**, 409 (1998).
[25]A. Hodgkin and A. Huxley, J. Physiol. **117**, 500 (1952).
[26]N. T. Carnevale and M. L. Hines, *The NEURON Book* (Cambridge University Press, New York, 2006).
[27]J. M. Bower and D. Beeman, *The Book of GENESIS: Exploring Realistic Neural Models With the General Neural Simulation System*, 2nd ed. (Springer, New York, 1998).
[28]W. Gerstner and W. M. Kistler, *Spiking Neuron Models* (Cambridge University Press, New York, 1999).
[29]N. F. Rulkov, Phys. Rev. Lett. **86**, 183 (2001).
[30]N. F. Rulkov, Phys. Rev. E **65**, 041922 (2002).
[31]D. R. Chialvo, Chaos, Solitons Fractals **5**, 461 (1995).
[32]M. Copelli, M. H. R. Tragtenberg, and O. Kinouchi, Physica A **342**, 263 (2004).
[33]E. M. Izhikevich, Int. J. Bifurcation Chaos **14**, 3847 (2004).
[34]M. V. Ivanchenko, G. V. Osipov, V. D. Shalfeev, and J. Kurths, Phys. Rev. Lett. **93**, 134101 (2004).
[35]Y. Kuramoto, *Chemical Oscillations, Waves and Turbulence* (Dover, New York, 2003).
[36]M. S. Baptista, H.-P. Ren, J. C. M. Swarts, R. Carareto, H. Nijmeijer, and C. Grebogi, PLoS ONE **7**, e48118 (2012).

[37]M. Steriade, D. A. McCormick, and T. J. Sejnowski, Science **262**, 679 (1993).
[38]L. B. Good, S. Sabesan, S. T. March, K. Tsakalis, D. Treiman, and L. Iasemidis, Int. J. Neural Syst. **19**, 173 (2009).
[39]A. Beuter, M. S. Titcombe, F. Richer, C. Gross, and D. Guehl, Thalamus Relat. Syst. **1**, 203 (2001).
[40]A. Beuter and M. S. Titcombe, Brain Cogn **53**, 190 (2003).
[41]M. S. Titcombe, L. Glass, D. Guehl, and A. Beuter, Chaos **11**, 766 (2001).
[42]J. Y. K. Lee and D. Kondziolka, J. Neurosurg. **103**, 400 (2005).
[43]A. S. Batista, A. M. Batista, J. A. C. de Pontes, R. L. Viana, and S. R. Lopes, Phys. Rev. E **76**, 016218 (2007).
[44]M. Rosenblum, N. Tukhlina, A. Pikowsky, and L. Cimponeriu, Int. J. Bifurcation Chaos **16**, 1989 (2006).
[45]C. A. S. Batista, E. L. Lameu, A. M. Batista, S. R. Lopes, T. Pereira, G. Zamora-López, J. Kurths, and R. L. Viana, Phys. Rev. E **86**, 016211 (2012).
[46]Y. Tang, Z. Wang, H. Gao, S. Swift, and J. Kurths, PLos ONE **7**, e41375 (2012).